ChemPubSoc Europe

DOI: 10.1002/open.201800287

Open Access ChemistryOPEN Full Papers

Synthesis of Non-Symmetrical Nitrogen-Containing Curcuminoids in the Pursuit of New Anticancer Candidates

Atiruj Theppawong,[a] Tim Van de Walle,[a] Charlotte Grootaert,[b] Kristof Van Hecke,[c] Nathalie Catry,[a] Tom Desmet,[d] John Van Camp,*[b] and Matthias D'hooghe*[a]

Curcumin is known to display pronounced anticancer effects and a variety of other biological activities. However, the low bioavailability and fast metabolism of this molecule present an issue of concern with respect to its medicinal applications. To address this issue, structural modifications of the curcumin scaffold can be envisioned as a strategy to improve both the solubility and stability of this chemical entity, without compromising its biological activities. Previous work in our group targeted the synthesis of symmetrical azaheteroaromatic curcuminoids, which showed better solubility and cytotoxicity profiles compared to curcumin. In continuation of that work, we now focused on the synthesis of non-symmetrical nitrogen-containing curcuminoids bearing both a phenolic and an azaheteroaromatic moiety. In that way, we aimed to combine good solubility, antioxidant potential and cytotoxic properties into one molecule. Some derivatives were selected for further chemical modification of their rather labile β-diketone scaffold to the corresponding pyrazole moiety. In this way, thirteen new non-symmetrical aza-aromatic curcuminoids and four pyrazole-based analogues were successfully synthesized in a yield of 11–69%. All newly synthesized analogues were evaluated for their antioxidant properties, reactive oxygen species (ROS) production, water solubility and anticancer activities. Several novel derivatives displayed good cytotoxicity profiles compared to curcumin, in combination with an improved water solubility and stability, and were thus identified as potential hit scaffolds for further optimization studies.

1. Introduction

Curcumin is an attractive compound with broad-spectrum activities and is still used as a folk medicine to treat a variety of illnesses such as liver disease (jaundice), indigestion, urinary tract diseases, rheumatoid arthritis, and insect irritation.[1] From a biological point of view, curcumin also exhibits a diversity of interesting properties including anticancer,[2] anti-inflammatory,[3] antioxidant,[4] antimicrobial[5] and antimalarial[6] activities. Moreover, curcumin has been shown to display a much stronger free-radical scavenger property than vitamin E,[2i,7] which is known for its antioxidant effects and other benefits in the human body. Considering these characteristics, curcumin could be considered as a suitable candidate for (anticancer) drug development. However, despite the aforementioned benefits, the clinical application of curcumin is severely limited because of its poor solubility and low stability/fast metabolism under physiological, both neutral and basic, conditions,[8] and curcumin has been classified as a PAINS (pan-assay interference compounds) and an IMPS (invalid metabolic panaceas) candidate.[9] In that respect, efforts to move away from the classical approaches in curcumin research (usually implying rather minor chemical modifications of the curcumin scaffold) are recommended, hence our focus on the pursuit of unprecedented types of nitrogen derivatives in the present study. In addition, curcumin extensively undergoes in vitro and in vivo Phase I and Phase II metabolism.[8a,10]

At present, multiple approaches are under investigation to overcome these limitations. For example, chemical modification of the curcumin structure has been studied and miscellaneous analogues have been synthesized to improve the therapeutic profile of the mother compound, curcumin. One advantage of developing molecules around the curcumin scaffold is the absence of toxicity, and it is believed that this unique property of curcumin is due to its selective cytotoxic activity to cancer cells only.[11] Surprisingly, large quantities of curcumin can be consumed without inflicting toxicity, up to 12 g per day.[12] Numerous analogues of curcumin have therefore been developed for therapeutic purposes to overcome the classical limitations. Chemically, the structure of curcumin is composed of two o-methoxy phenols, symmetrically attached at the two terminal positions of an α,β-unsaturated β-diketone linker, that

[a] A. Theppawong, T. Van de Walle, N. Catry, Prof. Dr. M. D'hooghe
SynBioC Research Group, Department of Green Chemistry and Technology, Faculty of Bioscience Engineering, Ghent University
Coupure Links 653, B-9000 Ghent, Belgium
E-mail: matthias.dhooghe@UGent.be
[b] Dr. C. Grootaert, Prof. Dr. J. Van Camp
Department of Food Technology, Safety and Health, Faculty of Bioscience Engineering, Ghent University
Coupure Links 653, B-9000 Ghent, Belgium
E-mail: john.vancamp@UGent.be
[c] Prof. Dr. K. Van Hecke
XStruct, Department of Chemistry, Faculty of Science, Ghent University
Krijgslaan 281, S3, B-9000 Ghent, Belgium
[d] Prof. Dr. T. Desmet
Department of Biotechnology,
Faculty of Bioscience Engineering, Ghent University
Coupure Links 653, 9000 Ghent, Belgium

Supporting information for this article is available on the WWW under https://doi.org/10.1002/open.201800287

©2019 The Authors. Published by Wiley-VCH Verlag GmbH & Co. KGaA. This is an open access article under the terms of the Creative Commons Attribution Non-Commercial NoDerivs License, which permits use and distribution in any medium, provided the original work is properly cited, the use is non-commercial and no modifications or adaptations are made.

stands in equilibrium with its enol tautomer.[13] In view of this, several research groups have attempted to modify these structural motifs of curcumin in order to slow down its metabolism and achieve improvements in the potency and efficacy of its anticancer activity.

To address the previously mentioned shortcomings, our former research focused on the synthesis of structurally modified nitrogen-containing curcumin analogues, such as β-enaminone and symmetrical azaheteroaromatic curcuminoids, in order to improve their bioavailability.[2h,i] Interestingly, many analogues exhibited good cytotoxicity profiles (low IC_{50} values) as compared to curcumin. The most polar compounds also showed much better water solubility than curcumin, albeit with a lower cytotoxicity. Thus, a good balance between cytotoxicity, water solubility and antioxidant properties must be pursued to deliver the best candidates for pharmaceutical applications. This work therefore focuses on the synthesis of non-symmetrical nitrogen-containing curcuminoids by introducing two different aryl groups in the curcumin framework, with at least one aryl group being azaheteroaromatic. Furthermore, some derivatives underwent an extra modification by converting the β-diketone moiety into its corresponding pyrazole framework. This cyclization leads to a more rigid structure and elimination of keto-enol tautomerism, making the resulting analogues less prone to Phase I/II metabolism.[10a,14] In that respect, some pyrazole curcuminoids have already been described in the literature as promising anticancer candidates.[14–15] For instance, one pyrazole analogue of curcumin was investigated for its lipoxygenase inhibitory activity[16] and three other pyrazole curcuminoids were evaluated with regard to endothelial cell proliferation and cytotoxicity.[17] In continuation of our previous work, these structural modifications should keep the pharmacodynamic profile of the new compounds on a similar (or improved) level as compared to curcumin. To validate the concept of our research, biological evaluation, water solubility and stability tests were conducted on all novel analogues and the results were compared to the results of their corresponding mother structures.

2. Results and Discussion

The synthetic procedure for the preparation of non-symmetrical curcuminoids is based on previously reported optimized conditions for the synthesis of curcumin and symmetrical curcumin analogues.[2i,18] In this work, however, two consecutive condensation reactions with different aldehydes had to be executed in order to obtain the desired non-symmetrical curcuminoids. In a first step, monoaryl curcumin analogues **2a–b** were synthesized using vanillin and indole-3-carboxaldehyde, respectively (Scheme 1). Vanillin was used to maintain the antioxidant properties associated with the ortho-methoxy phenol unit, while the rationale for using indole-3-carboxaldehyde is based on previous work, in which the symmetrical indol-3-yl curcuminoid showed promising features for further development. The optimized reaction conditions for both monoaryl analogues can be found in Table 1. Boron complexation with boron trioxide (B_2O_3) prevents the most acidic methylene protons to be deprotonated, and therefore avoids the formation of the Knoevenagel side product. The quantity of base applied in the reaction is based on color change of the reaction mixture from yellow to dark-brown. Careful monitoring via either TLC or LC-MS analysis was necessary to stop the reaction in time, although there was still starting material present (30–44%), in order to reach the highest conversion towards the desired monoaryl analogue with only minor formation (3–12%) of the symmetrical diaryl side product. The use of acetonitrile instead of ethyl acetate for the preparation of analogue **2b** resulted in a slightly higher yield. The crude reaction products were purified using reversed phase column chromatography to acquire monoaryl curcumin analogues **2a–b** in a yield of 32 and 30%, respectively.

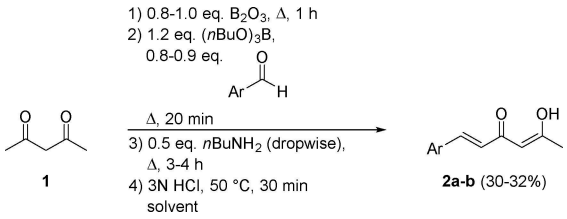

Scheme 1. Synthesis of monoaryl curcumin analogues **2a–b**.

Table 1. Reaction conditions and yields for the synthesis of monoaryl curcumin analogues **2a–b**.

Compd	Ar	Eq. B_2O_3	Eq. Ar	Yield (%)
2a	4-hydroxy-3-methoxyphenyl	0.8	0.9	32[a]
2b	indol-3-yl	1.0	0.8	30[b]

[a] in EtOAc for 4 h. [b] in MeCN for 3 h.

The obtained monoaryl curcumin analogues **2a–b** were subsequently deployed for the synthesis of non-symmetrical nitrogen-containing curcuminoids **3a–m** by means of a second condensation reaction with different azaheteroaromatic or thiaheteroaromatic (for derivative **3m**) aldehydes (Scheme 2, Figure 1). Table 2 displays the optimized reaction conditions for each analogue. As for the synthesis of monoaryl curcumin analogues **2a–b**, complexation with boron trioxide (B_2O_3) was again conducted to prevent the formation of the Knoevenagel side product. In comparison with the first condensation reaction, the amount of aldehyde was increased to more than one equivalent (1.1–1.5 equivalents), because full conversion of

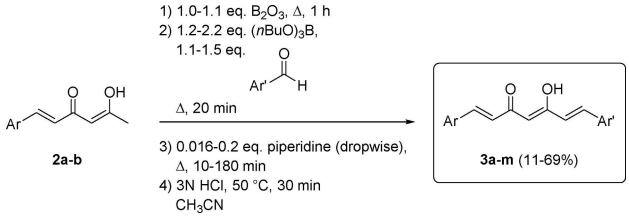

Scheme 2. Synthesis of non-symmetrical nitrogen-containing curcuminoids **3a–m**.

© 2019 The Authors. Published by Wiley-VCH Verlag GmbH & Co. KGaA

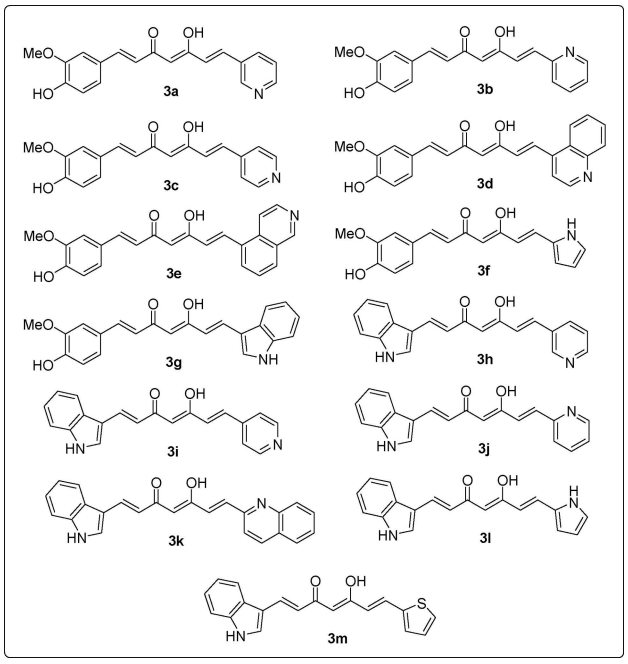

Figure 1. Non-symmetrical nitrogen-containing curcuminoids **3**.

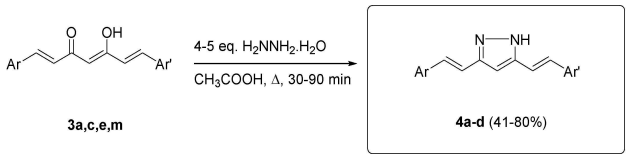

Scheme 3. Synthesis of pyrazole-based non-symmetrical nitrogen-containing curcuminoids **4a–d**.

Table 3. Reaction conditions and yields for the synthesis of pyrazole-based non-symmetrical nitrogen-containing curcuminoids **4a–d**.

Compd	Ar	Ar′	Eq. H_2NNH_2 H_2O	Time (min)	Yield (%)
4a	4-hydroxy-3-methoxyphenyl	pyridin-3-yl	5	60	75
4b	4-hydroxy-3-methoxyphenyl	pyridin-4-yl	4	30	79
4c	4-hydroxy-3-methoxyphenyl	isoquinolin-5-yl	5	90	41
4d	indol-3-yl	thiophen-2-yl	5	60	80

the starting material was desirable in this case. Also, piperidine seemed a better choice as base for the deprotonation of the terminal carbon atom of monoaryl analogues **2a–b**. A change in color of the reaction mixture again indicated the amount of base needed. It has been reported that piperidine can be used in low catalytic amounts to effect condensation reactions due to its high efficiency.[19] All reactions were followed up by either TLC or LC-MS analysis and stopped when full conversion was obtained. Only for analogues **3d**, **3e** and **3f**, a maximum conversion of approximately 80% could be reached. Purification of the crude products with the use of reversed phase column chromatography yielded non-symmetrical nitrogen-containing curcuminoids **3a–m** in 11–69% yield and high purity.

Four of the synthesized non-symmetrical curcuminoids (**3a**, **c**, **e**, **m**) were further modified and converted into their corresponding pyrazole-based derivatives. As mentioned before, this cyclization of the rather labile β-diketone moiety to a pyrazole scaffold renders more stable compounds for *in vitro* and *in vivo* metabolism and therefore, it is expected that this modification will lead to analogues with improved antiproliferative properties. Moreover, in previous literature studies, a pyrazole-based curcuminoids demonstrated interesting biological activity toward different cancer cells.[20] Scheme 3 shows the synthesis of pyrazole-based analogues **4a–d** through an acid-catalyzed condensation reaction with hydrazine hydrate. Based on a literature procedure, the reaction was first conducted in ethanol as solvent with a catalytic amount of acetic acid.[21] However, a switch to acetic acid as sole solvent resulted in faster conversion and higher yields. Full conversion was determined by means of either TLC or LC-MS analysis. Pyrazole-based non-symmetrical nitrogen-containing curcuminoids **4a–d** were obtained after purification *via* reversed phase column chromatography in a yield of 41–80% (Table 3, Figure 2). Moreover, a thiophen-2-yl curcuminoid (**5**) was synthesized (Figure 2, synthesis in supporting info) in order to compare its

Table 2. Reaction conditions and yields for the synthesis of non-symmetrical nitrogen-containing curcuminoids **3a-m**.

Compd	Ar	Ar′	Eq. B_2O_3	Eq. $(n\text{BuO})_3\text{B}$	Eq. Ar	Eq. piperidine	Time (min)[a]	Yield (%)
3a	4-hydroxy-3-methoxyphenyl	pyridin-3-yl	1.1	1.2	1.1	0.016	20	65
3b	4-hydroxy-3-methoxyphenyl	pyridin-2-yl	1.1	2.2	1.1	0.05	10	60
3c	4-hydroxy-3-methoxyphenyl	pyridin-4-yl	1.1	1.2	1.1	0.016	30	12
3d	4-hydroxy-3-methoxyphenyl	quinolin-4-yl	1.1	1.2	1.1	0.020	60	11
3e	4-hydroxy-3-methoxyphenyl	isoquinolin-5-yl	1.1	1.2	1.1	0.048	180	41
3f	4-hydroxy-3-methoxyphenyl	pyrrol-2-yl	1.0	2.2	1.2	0.1	90	37
3g	4-hydroxy-3-methoxyphenyl	indol-3-yl	1.1	2.2	1.2	0.2	10	49
3h	indol-3-yl	pyridin-3-yl	1.0	1.2	1.1	0.1	10	49
3i	indol-3-yl	pyridin-4-yl	1.0	1.2	1.1	0.1	15	16
3j	indol-3-yl	pyridin-2-yl	1.0	1.2	1.1	0.1	20	19
3k	indol-3-yl	quinolin-2-yl	1.0	1.2	1.1	0.15	30	43
3l	indol-3-yl	pyrrol-2-yl	1.0	1.2	1.1	0.2	60	62
3m	indol-3-yl	thiophen-2-yl	1.0	2.0	1.5	0.15	15	69

[a] Reaction time for step 3.

© 2019 The Authors. Published by Wiley-VCH Verlag GmbH & Co. KGaA

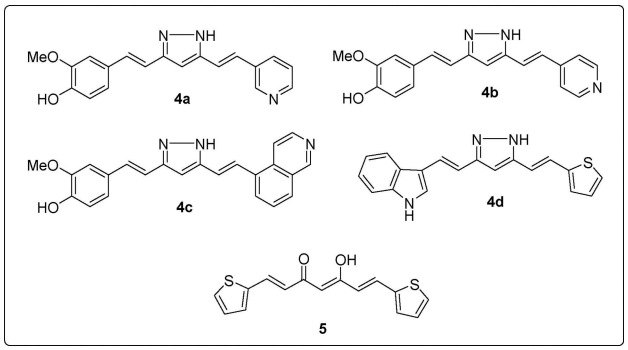

Figure 2. Pyrazole-based curcuminoids **4** and thiophen-2-yl curcuminoid **5**.

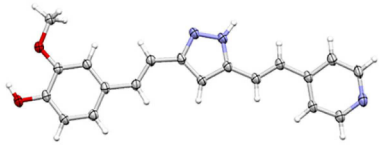

Figure 3. Molecular structure of **4b**, determined by X-ray analysis, showing thermal displacement ellipsoids at the 50% probability level.

bioactivity with compounds **3m** and **4d**, which contain one thiophen-2-yl moiety. X-ray analysis was used to confirm the structure of compound **4b** (Figure 3). In the structure of **4b**, dimers are formed through hydrogen bonds between two pyrazole rings (Figure S2, supporting info). These dimers are further hydrogen bonded into chains via hydrogen bonds between pyridine N-atoms and hydroxyl H-atoms (Figure S2, supporting info), leading to a typical herringbone crystal packing pattern (Figure S3, supporting info).

After we successfully obtained the desired products, we further investigated the physicochemical properties of these non-symmetrical curcuminoids. In that respect, water solubility tests were performed on all newly synthesized compounds following a similar procedure as in a previous research.[2h,i] An excess amount of solid was dissolved in 0.1 M phosphate buffer (pH 6.8) using the shake flask method.[22] The solubility values were obtained via linear regression of each standard curve, which was experimentally triplicated. In general, all azaheteroaromatic non-symmetrical analogues **3** (except **3e**) and pyrazole-based non-symmetrical compounds (**4**) showed better solubility than curcumin, their mother compound (Table 4). Moreover, the thiophenyl curcuminoid (**5**) also showed better solubility than **3d–e**, **h**, **m**, **4c** and curcumin (Table 4). From these results, we can conclude that through the synthesis of non-symmetrical analogues bearing at least one azaheteroaromatic moiety, we successfully achieved one of our main research aims, which was to produce new curcumin analogues with a better aqueous solubility. This higher aqueous solubility solves the problem of in vitro precipitation in biological medium.

Curcumin is also known to display interesting antioxidant properties.[23] To investigate the effect of our structural modifications on the antioxidant properties, two different series of non-symmetrical azaheteroaromatic curcumin analogues were designed. One series kept the ortho-methoxy phenol unit of curcumin, combined with an azaheteroaromatic part (**3a–g**), whereas in the other series (**3h–m**), the indol-3-yl moiety was used as fixed aromatic part and joined together with different azaheteroaromatics. The reason behind the applied structure modifications was to retain antioxidant/antiproliferative properties. All newly synthesized derivatives were assessed for their antioxidant effects using the ferric reducing antioxidant power (FRAP) assay.[2i,24] The FRAP assay is generally used to evaluate chemical antioxidant activity, which is expressed as either Trolox equivalents or curcumin equivalents. The known positive controls are α-tocopherol and ascorbic acid. Compounds **3a–g** showed around 50% reduced activity when compared to either curcumin or Trolox (**3c**, **f** showed activity comparable to ascorbic acid), whereas **3h–m** showed only 10–20% antioxidant properties compared to either curcumin or Trolox. Compounds **4a–d** illustrated 15–57% antioxidant properties compared to curcumin (**4a** showed effects comparable to ascorbic acid), which could be explained by the fact that the free NH functionality on either the indol-3yl moiety or on another azaheteroaromatic ring can be equipotent to the OH moiety on the curcumin scaffold in that respect. Thiophenyl curcuminoid (**5**) showed no interesting antioxidant properties (0.01 Trolox equivalent, 1% compared to curcumin). In other words, preservation of the 4-hydroxy-3-methoxyphenyl moiety (**3a–g**, **4a–c**) may provide interesting properties when combined with different azaheteroaromatics.

To evaluate anticancer properties, a combination of assays was performed in order to reveal essential information concerning these newly synthesized analogues (**3–5**). Compounds **3–5**

Table 4. Determination of solubility experiments in phosphate buffer (pH 6.8) and evaluation of chemical antioxidant capacity using FRAP assays, $n \geq 3$ triplicate independent experiments.

Compd	Solubility in 0.1 M phosphate buffer pH 6.8 (μM)		FRAP (Trolox equivalent per μM)	FRAP (curcumin equivalent per μM)
	90 min	24 h		
Cur	2.7 ± 0.1	2.6 ± 0.1	1.00	–
α-Tocopherol	N/A	N/A	0.70	0.68
Ascorbic acid	N/A	N/A	0.60	0.57
Trolox	N/A	N/A	–	1.00
3a	8.1 ± 1.6	14.5 ± 1.1	0.42	0.40
3b	9.9 ± 0.4	11.6 ± 0.6	0.41	0.40
3c	9.0 ± 0.6	12.8 ± 1.1	0.56	0.54
3d	3.6 ± 1.1	4.4 ± 1.3	0.20	0.20
3e	1.1 ± 0.2	1.4 ± 0.2	0.21	0.20
3f	20.9 ± 1.7	18.3 ± 0.4	0.56	0.54
3g	7.6 ± 0.9	13.2 ± 0.3	0.44	0.42
3h	5.3 ± 0.1	5.4 ± 0.1	0.13	0.12
3i	7.8 ± 0.1	7.7 ± 0.6	0.19	0.18
3j	10.7 ± 0.4	7.9 ± 0.2	0.16	0.15
3k	8.1 ± 0.1	9.6 ± 0.8	0.20	0.19
3l	12.2 ± 0.3	12.0 ± 0.7	0.29	0.27
3m	1.27 ± 0.0	1.25 ± 0.0	0.10	0.09
4a	8.8 ± 0.4	7.7 ± 0.7	0.57	0.55
4b	16.8 ± 1.6	12.8 ± 1.4	0.43	0.42
4c	6.4 ± 0.2	7.0 ± 0.2	0.15	0.14
4d	13.7 ± 0.5	11.7 ± 2.3	0.33	0.32
5	10.7 ± 0.2	12.8 ± 1.4	0.01	0.01

N/A: No analysis (commercially available compounds).

© 2019 The Authors. Published by Wiley-VCH Verlag GmbH & Co. KGaA

Table 5. Cell growth inhibition (expressed as IC_{50} values) of compounds **3–5** measured after 72 hours treatment as tested by mitochondrial activity (MTT) and protein content (SRB) assays.[a]

Compd	HepG2		HT-29		Caco-2		EA.hy926		CHO-K1	
	MTT (μM)	SRB (μM)	MTT (μM)	SRB (μM)	MTT (μM)	SRB (μM)	MTT (μM)	SRB (μM)	MTT (μM)	SRB (μM)
3a	14.1 ± 0.3	16.8 ± 0.9	17.9 ± 0.1	20.9 ± 0.9	14.6 ± 2.0	25.0 ± 1.8	8.5 ± 0.4	3.8 ± 0.0	21.4 ± 1.3	36.1 ± 1.3
3b	24.6 ± 4.8	20.6 ± 1.4	34.3 ± 2.7	34.8 ± 1.2	22.3 ± 0.9	25.8 ± 1.1	1.1 ± 0.1	3.1 ± 0.0	25.2 ± 1.5	30.9 ± 1.1
3c	3.2 ± 0.8	9.8 ± 0.6	4.9 ± 0.3	48.8 ± 1.8	7.1 ± 0.4	12.0 ± 0.7	6.1 ± 0.1	3.7 ± 0.2	13.3 ± 2.6	17.7 ± 1.4
3d	44.8 ± 5.5	55.4 ± 0.3	47.0 ± 1.0	47.2 ± 2.2	46.3 ± 3.7	40.8 ± 1.6	42.3 ± 1.2	60.2 ± 10.4	22.3 ± 1.4	19.3 ± 0.7
3e	4.7 ± 0.2	7.3 ± 0.3	1.3 ± 0.5	10.7 ± 1.6	6.9 ± 0.3	17.7 ± 3.0	5.2 ± 0.2	16.2 ± 0.6	7.6 ± 0.3	32.6 ± 0.4
3f	31.7 ± 0.6	7.1 ± 0.2	33.9 ± 0.4	36.1 ± 2.3	17.1 ± 0.4	15.9 ± 2.0	45.6 ± 0.9	33.8 ± 1.4	24.1 ± 1.6	49.0 ± 1.3
3g	19.5 ± 0.6	13.5 ± 1.1	12.9 ± 0.9	40.5 ± 4.3	5.8 ± 0.3	37.9 ± 1.8	19.0 ± 0.4	45.1 ± 2.6	26.4 ± 2.4	23.3 ± 3.3
3h	5.0 ± 0.3	10.2 ± 0.4	6.4 ± 0.8	34.6 ± 0.8	6.7 ± 0.4	10.3 ± 0.1	6.2 ± 0.3	2.9 ± 0.1	9.2 ± 0.6	24.3 ± 4.4
3i	48.5 ± 1.7	> 75	42.0 ± 1.0	64.2 ± 2.76	47.1 ± 1.6	29.8 ± 2.3	34.9 ± 1.3	> 75	42.9 ± 0.4	66.3 ± 6.3
3j	38.9 ± 0.8	34.0 ± 2.8	33.8 ± 3.5	46.0 ± 3.0	35.5 ± 0.4	40.2 ± 1.9	1.4 ± 0.2	3.7 ± 0.2	22.3 ± 1.2	34.7 ± 2.8
3k	56.2 ± 1.6	54.1 ± 1.0	42.0 ± 2.0	43.8 ± 0.9	44.7 ± 2.1	47.5 ± 0.2	38.3 ± 1.7	53.2 ± 1.3	41.6 ± 1.7	43.3 ± 0.4
3l	16.5 ± 0.4	9.8 ± 0.3	10.5 ± 0.1	10.0 ± 0.1	6.5 ± 0.2	10.1 ± 0.5	3.3 ± 0.1	4.2 ± 0.3	11.0 ± 0.5	9.64 ± 1.2
3m	4.7 ± 0.2	10.8 ± 1.6	6.9 ± 0.0	4.8 ± 0.3	0.5 ± 0.3	5.7 ± 0.2	4.4 ± 0.4	8.6 ± 0.5	5.9 ± 0.1	11.1 ± 0.4
4a	11.2 ± 0.1	> 75	> 75	24.0 ± 1.6	53.7 ± 6.1	18.7 ± 1.2	18.5 ± 1.3	60.7 ± 0.7	13.2 ± 0.7	13.6 ± 0.3
4b	56.7 ± 0.5	54.6 ± 0.3	49.0 ± 0.7	47.4 ± 0.2	39.3 ± 1.2	46.5 ± 0.5	35.7 ± 0.1	51.8 ± 0.3	32.2 ± 0.9	41.8 ± 0.7
4c	6.7 ± 0.4	28.3 ± 4.7	37.7 ± 1.3	> 75	58.7 ± 2.0	60.3 ± 3.5	38.8 ± 0.4	> 75	8.4 ± 0.0	7.9 ± 0.5
4d	34.9 ± 0.8	49.5 ± 2.1	4.2 ± 0.4	9.7 ± 0.5	19.6 ± 4.0	21.1 ± 0.3	6.0 ± 0.9	9.5 ± 0.4	0.9 ± 0.0	16.2 ± 1.0
5	> 75	66.0 ± 2.6	> 75	59.1 ± 3.3	42.0 ± 2.6	46.0 ± 0.9	43.7 ± 1.2	59.9 ± 1.5	44.0 ± 2.4	54.4 ± 4.1
Cur	25.3 ± 0.9	22.1 ± 2.6	43.4 ± 4.6	52.3 ± 3.8	47.6 ± 1.5	39.1 ± 0.1	46.8 ± 0.7	58.4 ± 4.2	44.9 ± 0.6	38.8 ± 0.3
Bis	17.8 ± 0.3	17.1 ± 1.0	49.7 ± 4.4	65.6 ± 5.2	17.3 ± 0.7	24.5 ± 3.3	17.2 ± 1.1	> 75	31.0 ± 2.5	31.0 ± 3.5
Dox	1.8 ± 0.1	1.3 ± 0.3	4.8 ± 0.1	2.7 ± 0.1	13.0 ± 0.5	9.2 ± 0.5	4.1 ± 0.1	3.4 ± 0.4	2.5 ± 0.1	2.4 ± 0.3

[a] Data are presented as mean ± standard deviation. Combination data of MTT and SRB ($n \geq 3$).

were evaluated for in vitro cytotoxicity against four cancer cell lines, HT-29, Caco-2, EAhy.926 and HepG2, and non-carcinoma cells (CHO-K1) by mitochondrial activity (MTT) and protein content (SRB) assays, as well as the measurement of intracellular reactive oxygen species (ROS) production. For the MTT and SRB assays, doxorubicin (Dox) was used as positive control and curcumin was taken as standard reference. In addition, *N*-acetyl-L-cysteine (NAC) and doxorubicin[25] were used as controls for respectively decreased and increased intracellular ROS production. The results are described as IC_{50} values in Table 5. From these results, it could be observed that most non-symmetrical analogues demonstrated higher mitochondrial activity compared to curcumin. Moreover, the SRB results pointed out a similar trend as the MTT results, and confirmed that azaheteroaromatic non-symmetrical analogues (**3a–m**) and pyrazole non-symmetrical analogues (**4a–d**) exerted stronger cell growth inhibition effects than curcumin. In contrast, compound **5** showed comparable activity to its mother compound, curcumin. Interestingly, compounds **3c**, **e**, **h**, **l** and **4c** even displayed comparable activity to the commercial doxorubicin drug. Previous work demonstrated that the introduction of azaheteroaromatic moieties leads to higher antiproliferative properties.[2i] Therefore, with the intention to combine antioxidant and antiproliferative properties, compounds **3–4** were designed in this work, and these compounds indeed showed an improved antiproliferative capacity, in addition to a better water solubility.

In the next set of experiments, intracellular ROS determination was performed in different cell lines in order to investigate their possible role in cytotoxicity-related pathways. An imbalance between ROS and antioxidants could lead to cell damage, which is implicated in a range of pathologies. Overproduction of reactive oxygen species is considered as toxic and will sequentially cause damage to lipids, proteins and DNA, which could further increase the risk of cancer development.[26] Moreover, higher ROS production may trigger cell apoptosis pathways by stimulating intrinsic mitochondrial pathways.[27] The experiment was conducted using 2′,7′-dichlorodihydrofluorescein diacetate (DCFH-DA). Two concentrations (10 and 1 μM) were examined, parallel with previous work.[2g–i] Moreover, ROS data were normalized on SRB measurements of the same well, in order to correct for differences in cell density. One of the controls in these experiments was NAC, a ROS inhibitor,[28] which induced a significant decrease in ROS generation in four different cancer cell lines, namely HepG2, HT-29, Caco-2 and EA.hy926, which was also observed in previous research.[2i] Moreover, doxorubicin induced a significant increase in ROS generation in all five cell lines. Both decreased and increased intracellular ROS levels were observed, and this was compound and cell line dependent (Table 6). In the HepG2 cell line, compounds **3a** and **4c** showed a significantly decreased ROS signal, whereas compounds **3c**, **f**, **h**, **i**, **k–m**, **4b** and **4d** exhibited a significantly increased ROS production. In the HT-29 cell line, compounds **3a**, **d–e**, **g–i** and **4a** showed a significantly decreased ROS signal, whereas compounds **3f**, **k–m**, **4d** and **5** showed a higher ROS signal. In the Caco-2 cell line, compounds **3e** and **4a** showed significantly decreased ROS production, whereas compounds **3a**, **f–g**, **k–m**, **4d** and **5** showed significantly increased ROS production, which have similar trends concerning intestinal carcinoma, represented by the HT-29 cell line. In the EA.hy926 cell line, only **4b** showed decreased intracellular ROS, whereas compounds **3a–b**, **d–e**, **f–g**, **i–m** and **4d** showed significantly increased ROS production. In the CHO-K1 cell line, only **5** showed decreased intracellular ROS, whereas compounds **3b–c**, **d**, **f**, **h**, **j–m**, **4b** and **d** showed significantly increased ROS. The ROS reduction effects were

© 2019 The Authors. Published by Wiley-VCH Verlag GmbH & Co. KGaA

Table 6. Intracellular ROS, expressed as percentage compared to the untreated control cells ($n \geq 3$) with protein content normalization (ROS/SRB).[a]

Compd	HepG2		HT-29		Caco-2		EA.hy926		CHO-K1	
	10 μM	1 μM	10 μM	1 μM	10 μM	1 μM	10 μM	1 μM	10 μM	1 μM
3a	82.3 ± 1.9**	116.0 ± 12.8	89.9 ± 4.3*	83.2 ± 3.2*	119.8 ± 8.7*	106.4 ± 8.4	95.5 ± 5.1	123.0 ± 9.5*	105.1 ± 3.8	99.7 ± 2.3
3b	91.9 ± 9.2	108.0 ± 6.7	93.6 ± 3.1	80.8 ± 2.5	99.7 ± 6.2	92.7 ± 5.4	127.2 ± 4.9*	100.5 ± 7.0	114.9 ± 6.15*	114.2 ± 7.4
3c	128.3 ± 4.4*	103.9 ± 13.1	99.8 ± 11.4	93.4 ± 6.4	99.7 ± 1.0	89.8 ± 3.6	95.7 ± 3.5	100.4 ± 6.9	129.1 ± 6.8*	100.0 ± 11.0
3d	99.6 ± 11.7	90.7 ± 7.4	96.9 ± 8.0	71.3 ± 4.9*	107.8 ± 4.4	94.2 ± 5.0	131.8 ± 6.5*	95.6 ± 7.0	119.9 ± 3.2**	95.1 ± 9.2
3e	96.7 ± 4.3	103.3 ± 5.1	67.6 ± 5.1*	80.6 ± 4.8	72.7 ± 5.1*	92.8 ± 11.9	120.1 ± 4.4*	96.3 ± 4.3	98.5 ± 3.6	94.9 ± 6.3
3f	216.3 ± 13.7*	98.9 ± 2.9	109.2 ± 2.6*	117.4 ± 10.5	146.8 ± 12.0*	124.8 ± 3.5*	131.7 ± 12.7*	125.1 ± 9.7*	111.7 ± 2.3*	113.0 ± 1.5*
3g	104.3 ± 12.0	110.7 ± 14.5	90.4 ± 5.1	85.7 ± 1.3*	110.6 ± 3.1*	102.3 ± 11.3	92.7 ± 6.1	128.8 ± 9.2*	97.0 ± 4.0	94.7 ± 4.0
3h	111.6 ± 4.9*	114.9 ± 4.5*	95.6 ± 4.2	82.3 ± 1.5*	127.6 ± 8.2*	111.0 ± 3.2*	106.6 ± 5.3	97.9 ± 9.8	106.8 ± 1.5	119.6 ± 3.8*
3i	146.7 ± 12.8*	124.9 ± 12.0*	73.6 ± 5.3*	73.3 ± 7.8*	89.7 ± 8.9	101.2 ± 5.1	118.9 ± 2.9*	105.9 ± 10.5	104.6 ± 6.6	86.9 ± 12.9
3j	96.6 ± 5.9	92.6 ± 6.5	101.7 ± 6.4	114.3 ± 15.5	84.9 ± 7.0	98.2 ± 2.6	110.8 ± 3.5*	90.8 ± 2.4	126.3 ± 4.1**	103.9 ± 0.38
3k	197.4 ± 24.6**	156.0 ± 13.0**	116.2 ± 7.1*	111.8 ± 10.8	168.2 ± 28.1*	162.4 ± 21.7*	126.2 ± 5.6*	120.2 ± 9.2	234.0 ± 12.0*	192.8 ± 14.1*
3l	997.7 ± 60.2**	600.0 ± 61.8*	558.0 ± 96.3*	152.5 ± 8.8*	767.2 ± 4.1**	410.1 ± 31.9 **	826.5 ± 22.7**	438.0 ± 46.1*	135.4 ± 10.7*	126.6 ± 10.5*
3m	424.4 ± 28.4**	317.5 ± 13.2**	336.6 ± 22.0**	247.2 ± 15.5**	295.1 ± 11.1**	238.2 ± 5.5**	321.5 ± 9.6**	344.3 ± 7.1**	146.9 ± 8.1*	138.6 ± 12.9*
4a	83.1 ± 5.5	88.4 ± 6.3	84.8 ± 3.8	61.3 ± 6.9*	86.7 ± 2.0	79.1 ± 8.8*	97.3 ± 7.3	90.6 ± 6.8	103.2 ± 8.9	96.6 ± 17.0
4b	123.4 ± 11.4*	135.0 ± 14.1*	113.7 ± 12.3	110.8 ± 16.2	94.3 ± 6.7	106.5 ± 4.6	80.6 ± 6.8*	86.9 ± 1.6*	144.6 ± 11.6*	100.9 ± 7.4
4c	88.0 ± 10.6	74.7 ± 2.9**	86.4 ± 8.2	94.4 ± 3.4	102.5 ± 17.3	107.8 ± 18.6	99.2 ± 5.0	89.9 ± 2.5	95.5 ± 3.7	102.8 ± 7.1
4d	984.7 ± 78.2*	1242.3 ± 65.7*	383.5 ± 47.5*	463.3 ± 42.7*	381.8 ± 62.6*	457.8 ± 97.5*	402.1 ± 23.4*	483.9 ± 1.4**	1038.8 ± 72.1*	797.4 ± 77.7*
5	110.4 ± 10.4	107.6 ± 9.4	134.8 ± 10.4*	111.0 ± 14.8	137.8 ± 14.2*	133.5 ± 12.4*	104.9 ± 8.0	97.3 ± 11.3	78.8 ± 3.1*	93.1 ± 11.3
Cur	100.9 ± 8.8	90.8 ± 12.0	86.5 ± 4.5*	106.1 ± 8.4	114.6 ± 7.2*	130.8 ± 3.6**	97.6 ± 5.7	100.5 ± 7.7	101.4 ± 2.1	102.6 ± 4.0
Bis	175.2 ± 6.5**	137.7 ± 17.7	112.0 ± 10.4	117.2 ± 3.5*	157.6 ± 11.4*	102.1 ± 11.0	126.6 ± 9.2	101.3 ± 8.7	136.7 ± 18.5	107.7 ± 2.5
Dox	118.8 ± 4.2*	100.5 ± 4.1	125.7 ± 1.8*	116.4 ± 1.7*	112.1 ± 3.9*	120.8 ± 9.4*	124.6 ± 5.1*	107.5 ± 6.2	129.1 ± 5.2*	145.7 ± 19.0*
NAC	63.1 ± 4.3**	77.1 ± 7.8*	75.3 ± 3.3*	82.7 ± 3.4*	83.5 ± 5.1*	83.7 ± 6.2*	76.6 ± 8.3*	84.2 ± 4.8*	100.1 ± 3.4	99.7 ± 2.3

[a] Data are presented as mean ± standard deviation; $n \geq 3$. *$p < 0.05$, **$p < 0.001$ indicate significant increase or decrease compared to the untreated control cells according to a two-tailed student-test with unequal variances.

© 2019 The Authors. Published by Wiley-VCH Verlag GmbH & Co. KGaA

Open Access ChemistryOPEN Full Papers

related to the compounds that contained the 4-hydroxy-3-methoxyphenyl moiety (**3a–g**), which demonstrated approximately 50% antioxidant properties in comparison with curcumin based on the FRAP assay (Table 4). Moreover, non-symmetrical curcuminoids with an indol-3yl aromatic moiety (**3h–m**) induced higher intracellular ROS production, especially compounds **3k–m** showing promising results in this work, despite their 13–30% antioxidant properties based on the FRAP assay. Results from our previous work also announced higher ROS productions in pyrol-2yl and indol-3yl curcuminoid analogues,[2i] with similar trends as azaheteroaromatic non-symmetrical derivatives 3 h–m. Therefore, our data for **3h–m** showed pro-oxidative effects of non-symmetrical derivatives. As we compared the results with the positive controls (Dox), the increased ROS production was observed in the non-symmetrical indol-3-yl curcuminoids (**3h–m**) and **3f–g**, which may undergo similar intrinsic mitochondrial pathways leading to cell apoptosis. However, some compounds showed different pro-oxidative and antioxidative effects depending on the cell characteristics. For instance, HepG2 are liver cancer cells which display robustness and a detoxification mechanism,[29] whereas intestinal cells serve two main functions: absorbing useful substances into the body and restricting the entry of harmful substances.[30]

3. Conclusions

In summary, we successfully produced thirteen new non-symmetrical nitrogen-containing curcuminoids, four pyrazole-based curcuminoids and one thiophen-2-yl curcuminoid. To obtain the desired derivatives, the synthesis started from monoaryl curcuminoids **2a–b** (4-hydroxy-3-methoxyphenyl for **3a–g** and indol-3-yl for **3h–m**). The preparation was performed by complexation of either **2a** or **2b**, followed by a condensation reaction with other aldehydes in order to furnish the expected compounds in moderate to good yields. Furthermore, the β-diketo functionality in some derivatives was transformed into the corresponding pyrazole moiety, resulting in compounds **4a–d**. All synthesized compounds (**3–5**) demonstrated improved water solubility when compared to curcumin, their mother compound. In this study, several new analogues showed a good bio-accessibility as expressed by improved water solubility and cytotoxicity (MTT and SRB, low IC_{50} values). Compounds **3–4** exhibited notably good antiproliferative activity towards different cancer cell lines (HepG2, HT-29, Caco-2 and EA.hy926) compared to curcumin. On the basis of our analysis, the azaheteroaromatic non-symmetrical curcuminoids showed higher solubility (2–7 fold) than curcumin. Compounds **3a**, **c**, **e**, **g–h**, **l–m**, **4a**, and **4c–d** demonstrated good antiproliferative activities towards four different cell lines (HepG2, EA.hy926, HT-29 and Caco-2). Furthermore, activity against non-carcinogenic cells (CHO-K1) mostly showed higher IC_{50} values as compared to carcinogenic cancer cell lines, which implied that newly synthesized compounds may be less harmful towards healthy cells. Therefore, these non-symmetrical analogues offer a desirable balance between good physicochemical properties and remarkable bioactivities, and thus represent interesting hit compounds for further in depth investigations.

Experimental Section

Chemistry

^{1}H NMR spectra were recorded at 400 MHz (Bruker Avance III Nanobay) with $CDCl_3$, DMSO-*d6* or MeOD-*d4* as solvent. ^{13}C NMR spectra were recorded at 100.6 MHz (Bruker Avance III Nanobay) with $CDCl_3$, DMSO-*d6* or MeOD-*d4* as solvent. Low resolution mass spectra were recorded via injection on an Agilent 1100 Series LC/MSD type SL mass spectrometer with electrospray ionization (ESI 70 eV) and using a mass-selective detector (quadrupole). When crude reaction mixtures were analyzed, the mass spectrometer was preceded by a HPLC reversed phase column (Ascentis® Express C18, HPLC column 3 cm × 4.6 mm, 2.7 μm) with a diode array UV/VIS detector. IR spectra were measured with a Fourier Transform Infrared spectrophotometer (The IRaffinity-1S). Melting points of crystalline compounds were measured with a Kofler Bench, type WME Heizbank of Wagner & Munz. The purity of all tested compounds was assessed by ^{1}H NMR analysis and/or HPLC analysis, confirming a purity of ≥ 95%.

Representative Procedure for the Synthesis of Monoaryl Curcumin Analogues 2a–b

The synthesis of (1*E*,4*Z*)-5-hydroxy-1-(4-hydroxy-3-methoxyphenyl) hexa-1,4-diene-3-one **2a** will be described as a representative example for the synthesis of monoaryl curcumin analogues **2a–b**. The reaction conditions for monoaryl analogue **2b** can be found in Table 1.

Acetylacetone (1; 40 mmol, 4.11 mL) was added to a solution of 0.8 equivalents boron trioxide (32 mmol, 2.23 g) in ethyl acetate (30 mL). The mixture was stirred at reflux for 1 h. Then, 0.9 equivalents vanillin (36 mmol, 5.48 g) and 1.2 equivalents tributyl borate (48 mmol, 12.95 mL) were added and the reaction mixture was stirred for an additional 20 min at reflux conditions. Afterwards, 0.5 equivalents of n-butylamine (20 mmol, 1.98 mL) were added dropwise. The reaction mixture was further stirred for 4 h at reflux conditions until maximum conversion was reached according to either TLC or LC-MS analysis. After cooling down to 50 °C, decomplexation of the boron complex was performed by adding 15 mL 1 N HCl to the reaction mixture and letting it stir for 30 min. The reaction was washed with a saturated solution of sodium bicarbonate (3 × 30 mL), after which the aqueous phase was extracted with ethyl acetate (3 × 30 mL). The combined organic fractions were washed with H_2O and brine and then dried with magnesium sulphate, filtrated and evaporated under reduced pressure. Purification by reversed phase column chromatography (acetonitrile/water, gradient conditions from 15 to 100%) yielded (1*E*,4*Z*)-5-hydroxy-1-(4-hydroxy-3-methoxyphenyl)hexa-1,4-diene-3-one **2a** (2.70 g, 32%).

For both monoaryl curcumin analogues **2a–b**, the obtained spectra corresponded with those described in the literature.[31]

Representative Procedure for the Synthesis of Non-Symmetrical Nitrogen-Containing Curcuminoids 3a–m.

The synthesis of (1*E*,4*Z*,6*E*)-5-hydroxy-1-(4-hydroxy-3-methoxyphenyl)-7-(pyridin-3-yl)hepta-1,4,6-triene-3-one **3a** will be described as a representative example for the synthesis of non-symmetrical nitro-

© 2019 The Authors. Published by Wiley-VCH Verlag GmbH & Co. KGaA

gen-containing curcuminoids **3a–m**. The reaction conditions for analogues **3b–m** can be found in Table 2.

(1*E*,4*Z*)-5-Hydroxy-1-(4-hydroxy-3-methoxyphenyl)hexa-1,4-diene-3-one **2a** (1 mmol, 234.25 mg) was added to a solution of 1.1 equivalents boron trioxide (1.1 mmol, 76.58 mg) in acetonitrile (10 mL) at reflux. After stirring for 1 h at reflux, 1.1 equivalents pyridin-3-carboxaldehyde (1.1 mmol, 0.10 mL) and 1.2 equivalents tributyl borate (1.2 mmol, 0.32 mL) were added. The reaction mixture was stirred for 20 min, after which 0.016 equivalents piperidine (0.016 mmol, 0.0016 mL), dissolved in acetonitrile (1:10), were added. After 20 min of stirring at reflux conditions, full conversion was determined by either TLC or LC-MS analysis, and the reaction mixture was cooled down to 50 °C. 3 N HCl (0.5 mL) was added and the mixture was stirred during 30 min at 50 °C. The reaction mixture was washed with a saturated solution of sodium bicarbonate (3×10 mL), after which the aqueous phase was extracted with ethyl acetate (3×10 mL). The combined organic fractions were washed with H_2O and brine. Then, the solution was dried over $MgSO_4$, filtrated and evaporated under reduced pressure. After reversed phase column chromatography (acetonitrile/water, gradient conditions from 15 to 100%), (1*E*,4*Z*,6*E*)-5-hydroxy-1-(4-hydroxy-3-methoxyphenyl)-7-(pyridin-3-yl)hepta-1,4,6-triene-3-one **3a** (210.18 mg, 65%) could be obtained.

(1*E*,4*Z*,6*E*)-5-Hydroxy-1-(4-hydroxy-3-methoxyphenyl)-7-(pyridin-3-yl)hepta-1,4,6-triene-3-one (**3a**): orange solid (65%); reversed phase column chromatography, t_R = 3.31 min (gradient conditions, 15% acetonitrile in water to 100% acetonitrile, 5 min, flow rate: 1 mLmin^{-1}); ^{1}H NMR (400 MHz, $CDCl_3$): δ = 3.96 (3H, s), 5.85 (1H, s), 6.51 (1H, d, *J* = 15.7 Hz), 6.67 (1H, d, *J* = 15.9 Hz), 6.94 (1H, d, *J* = 8,1 Hz), 7.06 (1H, d, *J* = 1.5 Hz); 7.14 (1H, dd, *J* = 8.1, 1.5 Hz), 7.34 (1H, dd, *J* = 7.9, 4.8 Hz), 7.62 (1H, d, *J* = 15.9 Hz), 7.63 (1H, d, *J* = 15.7 Hz), 7.85 (1H, dt, *J* = 7.9, 1.7 Hz), 8.59 (1H, dd, *J* = 4.8, 1.7 Hz), 8.78 ppm (1H, d, *J* = 1.7 Hz); ^{13}C NMR (100 MHz, $CDCl_3$): δ = 56.0, 101.8, 109.7, 114.9, 121.7, 123.2, 123.8, 125.9, 127.4, 130.9, 134.2, 136.1, 141.7, 146.9, 148.2, 149.5, 150.5, 180.4, 185.4 ppm; IR (ATR): ν 2924 (br), 1624, 1508, 1429, 1273, 1213, 1179, 1125 cm^{-1}; MS (70 eV): m/z (%) = 324 $[M+1]^+$ (46), 102 (40), 86 (100); Mp = 195 °C.

(1*E*,4*Z*,6*E*)-5-Hydroxy-1-(4-hydroxy-3-methoxyphenyl)-7-(pyridin-2-yl)hepta-1,4,6-triene-3-one (**3b**): Orange solid (60%); reversed phase column chromatography, t_R = 3.42 min (gradient conditions, 15% acetonitrile in water to 100% acetonitrile, 5 min, flow rate: 1 mLmin^{-1}); 1H NMR (400 MHz, $CDCl_3$): δ = 3.88 (3H, s), 5.83 (1H, s), 6.47 (1H, d, *J* = 15.7 Hz), 6.90 (1H, d, *J* = 8.0 Hz), 7.03 (1H, s), 7.08 (1H, d, *J* = 8.0 Hz), 7.12 (1H, d, *J* = 15.5 Hz), 7.23 (1H, dd, *J* = 7.5, 4.7 Hz), 7.38 (1H, d, *J* = 7.5 Hz), 7.58 (1H, d, *J* = 15.7 Hz), 7.59 (1H, d, *J* = 15.5 Hz), 7.69 (1H, td, *J* = 7.5, 1.3 Hz), 8.62 ppm (1H, dd, *J* = 4.7, 1.3 Hz); 13 C NMR (100 MHz, CDCl3): δ = 56.0, 102.6, 109.8, 115.2, 122.0, 123.4, 124.0, 124.8, 127.4, 127.9, 137.0, 138.0, 141.9, 147.2, 148.5, 150.1, 153.5, 179.7, 186.6 ppm; IR (ATR): ν 3065 (br), 1628, 1584, 1510, 1468, 1429, 1132, 970 cm^{-1}; MS (70 eV): m/z (%) = 324 $[M+1]^+$ (100); Mp = 162 °C.

(1E,4Z,6E)-5-Hydroxy-1-(4-hydroxy-3-methoxyphenyl)-7-(pyridin-4-yl)hepta-1,4,6-triene-3-one (**3c**): Dark-orange solid (12%); reversed phase column chromatography, t_R = 3.32 min (gradient conditions, 15% acetonitrile in water to 100% acetonitrile, 5 min, flow rate: 1 mLmin^{-1}); ^{1}H NMR (400 MHz, $CDCl_3$): δ = 3.96 (3H, s), 5.87 (1H, s), 6.52 (1H, d, *J* = 15.8 Hz), 6.75 (1H, d, *J* = 16.0 Hz), 6.95 (1H, d, *J* = 8.2 Hz), 7.07 (1H, d, *J* = 1.8 Hz), 7.15 (1H, dd, *J* = 8.2, 1.8 Hz), 7.38 (2H, dd, *J* = 4.6, 1.4 Hz), 7.54 (1H, d, *J* = 16.0 Hz), 7.65 (1H, d, *J* = 15.8 Hz), 8.65 ppm (2H, dd, *J* = 4.6, 1.4 Hz); ^{13}C NMR (100 MHz, $CDCl_3$): δ = 56.0, 102.3, 109.7, 114.9, 121.7, 121.8, 123.3, 127.4, 128.1, 136.6, 142.1, 142.4, 146.8, 148.3, 150.6, 179.1, 186.5 ppm; IR (ATR): ν 2928 (br), 1624, 1593, 1512, 1423, 1281, 1251, 1126 cm^{-1}; MS (70 eV): m/z (%) = 324 $[M+1]^+$ (100); Mp = 210 °C.

(1*E*,4*Z*,6*E*)-5-Hydroxy-1-(4-hydroxy-3-methoxyphenyl)-7-(quinolin-4-yl)hepta-1,4,6-triene-3-one (**3d**): Dark-orange solid (11%); reversed phase column chromatography, t_R = 3.12 min (gradient conditions, 15% acetonitrile in water to 100% acetonitrile, 5 min, flow rate: 1 mLmin^{-1}); ^{1}H NMR (400 MHz, $CDCl_3$): δ = 3.96 (3H, s), 5.92 (1H, s), 6.55 (1H, d, *J* = 15.8 Hz), 6.81 (1H, d, *J* = 15.6 Hz), 6.95 (1H, d, *J* = 8.2 Hz), 7.08 (1H, d, *J* = 1.7 Hz), 7.16 (1H, dd, *J* = 8.2, 1.7 Hz); 7.58 (1H, d, *J* = 4.5 Hz), 7.62–7.66 (1H, m), 7.67 (1H, d, *J* = 15.8 Hz), 7.75–7.80 (1H, m), 8.16 (1H, d, *J* = 8.4 Hz), 8.22 (1H, d, *J* = 8.4 Hz), 8.37 (1H, d, *J* = 15.6 Hz), 8.95 ppm (1H, d, *J* = 4.5 Hz); ^{13}C NMR (100 MHz, $CDCl_3$): δ = 56.0, 102.4, 109.7, 114.9, 117.8, 121.8, 123.4, 123.5, 126.2, 127.2, 127.4, 129.8, 129.9, 130.2, 133.8, 140.8, 142.2, 146.9, 148.3, 148.8, 150.1, 179.0, 186.6 ppm; IR (ATR): ν 2922 (br), 1626, 1580, 1508, 1425, 1273, 1209, 1125, 1030, 962, 758 cm^{-1}; MS (70 eV): m/z (%) = 374 $[M+1]^+$(100); Mp = 192 °C.

(1*E*,4*Z*,6*E*)-5-Hydroxy-1-(4-hydroxy-3-methoxyphenyl)-7-(isoquinolin-5-yl)hepta-1,4,6-triene-3-one (**3e**): Light-brown solid (41%); reversed phase column chromatography, t_R = 3.53 min (gradient conditions, 15% acetonitrile in water to 100% acetonitrile, 5 min, flow rate: 1 mLmin^{-1}); ^{1}H NMR (400 MHz, $CDCl_3$): δ = 3.96 (3H, s), 5.89 (1H, s), 6.53 (1H, d, *J* = 15.7 Hz), 6.73 (1H, d, *J* = 15.6 Hz), 6.95 (1H, d, *J* = 8.3 Hz), 7.07 (1H, d, *J* = 1.7 Hz), 7.15 (1H, dd, *J* = 8.2, 1.7 Hz), 7.63–7.67 (2H, m), 7.65 (1H, d, *J* = 15.7 Hz), 8.01–8.04 (3H, m), 8.37 (1H, d, *J* = 15.6 Hz), 8.63 (1H, d, *J* = 6.1 Hz), 9.29 ppm (1H, s); ^{13}C NMR (100 MHz, $CDCl_3$): δ = 56.0, 102.0, 109.7, 114.9, 116.4, 121.8, 123.2, 126.9, 127.4, 127.5, 128.5, 128.9, 129.6, 131.7, 134.2, 134.7, 141.6, 143.9, 146.9, 148.2, 153.3, 180.7, 185.4 ppm; IR (ATR): ν 2924 (br), 1626, 1582, 1510, 1283, 1136 cm^{-1}; MS (70 eV): m/z (%) = 374 $[M+1]^+$ (100), 396 $[M+Na]^+$(10); Mp = 204 °C.

(1*E*,4*Z*,6*E*)-5-Hydroxy-1-(4-hydroxy-3-methoxyphenyl)-7-(1*H*-pyrrol-2-yl)hepta-1,4,6-trien-3-one (**3f**): dark-red solid (37%); reversed phase column chromatography, t_R = 3.43 min (gradient conditions, 15% acetonitrile in water to 100% acetonitrile, 5 min, flow rate: 1 mLmin^{-1}); ^{1}H NMR (400 MHz, [D_4]MeOD): δ = 3.90 (s, 3H), 5.84 (s, 1H), 6.23 (dd, *J* = 3.3, 2.4 Hz, 1H), 6.36 (d, *J* = 15.7 Hz, 1H), 6.56–6.60 (m, 2H), 6.82 (d, *J* = 8.2 Hz, 1H), 6.98 (dd, *J* = 2.4, 1.2 Hz, 1H), 7.09 (dd, *J* = 8.2, 1.7 Hz, 1H), 7.19 (d, *J* = 1.7 Hz, 1H), 7.52 ppm (dd, *J* = 15.7, 4.5 Hz, 2H); ^{13}C NMR (100 MHz, [D_4]MeOD): δ = 55.0, 100.4, 110.2, 110.3, 114.8, 115.2, 116.78, 116.81, 120.7, 120.8, 122.5, 123.2, 127.3, 129.3, 130.9, 140.0, 148.0, 148.8, 181.26, 181.32, 185.0, 185.1 ppm; IR (ATR): ν 3296 (br), 1620, 1566, 1508, 1425, 1261, 1157 cm^{-1}; MS (70 eV): m/z (%) = 312 $[M+1]^+$(100), 334 $[M+Na]^+$ (80); Mp = 162 °C.

(1*E*,4*Z*,6*E*)-5-Hydroxy-1-(4-hydroxy-3-methoxyphenyl)-7-(1*H*-indol-3-yl)hepta-1,4,6-trien-3-one (**3g**): dark red solid (49%); reversed phase column chromatography, t_R = 3.51 min (gradient conditions, 15% acetonitrile in water to 100% acetonitrile, 5 min, flow rate: 1 mLmin^{-1}); ^{1}H NMR (400 MHz, $CDCl_3$): δ = 3.95 (s, 3H), 5.82 (s, 1H), 5.87 (brs, 1H), 6.49 (d, *J* = 15.8 Hz, 1H), 6.69 (d, *J* = 15.8 Hz, 1H), 6.94 (d, *J* = 8.2 Hz, 1H), 7.05 (d, *J* = 1.6 Hz, 1H), 7.12 (dd, *J* = 8.2, 1.6 Hz, 1H), 7.27–7.32 (m, 2H), 7.42–7.45 (m, 2H), 7.54 (d, *J* = 2.4 Hz, 1H), 7.58 (d, *J* = 15.8 Hz, 1H), 7.94 (d, *J* = 15.8 Hz, 1H), 7.94–7.98 (m, 1H), 8.54 ppm (brs, 1H); 13 C NMR (100 MHz, CDCl3): δ = 56.0, 101.1, 109.5, 111.9, 114.5, 114.8, 120.2, 120.6, 121.6, 121.8, 122.7, 123.5, 125.4, 127.9, 129.1, 134.6, 137.2, 139.7, 146.8, 147.6, 181.6, 185.3 ppm ; IR (ATR): ν 3336 (br), 1566, 1508, 1454, 1423, 1242, 1124 cm^{-1}; MS (70 eV): m/z (%) = 362 $[M+1]^+$(100); Mp = 174 °C.

(1*E*,4*Z*,6*E*)-5-Hydroxy-1-(1*H*-indol-3-yl)-7-(pyridin-3-yl)hepta-1,4,6-trien-3-one (**3h**): orange solid (49%); reversed phase column chromatography, t_R = 3.45 min (gradient conditions, 15% acetonitrile in water to 100% acetonitrile, 5 min, flow rate: 1 mLmin^{-1}); ^{1}H NMR (400 MHz, [D_6]DMSO): δ = 6.20 (s, 1H), 6.82 (d, *J* = 15.8 Hz, 1H), 7.02 (d, *J* = 16.0 Hz, 1H), 7.20–7.27 (m, 2H), 7.46 (dd, *J* = 7.9, 4.4 Hz, 1H), 7.50 (dd, *J* = 6.8, 1.7 Hz, 1H), 7.60 (d, *J* = 16.0 Hz,

© 2019 The Authors. Published by Wiley-VCH Verlag GmbH & Co. KGaA

1H), 7.99 (d, J = 15.8 Hz, 1H), 8.02 (d, J = 1.4 Hz, 1H), 8.03 (s, 1H), 8.15 (d, J = 7.9 Hz, 1H), 8.57 (d, J = 4.4 Hz, 1H), 8.88 (s, 1H), 11.93 ppm (brs, 1H); ^{13}C NMR (100 MHz, [D$_6$]DMSO): δ = 102.1, 113.0, 113.2, 118.5, 120.7, 121.6, 123.3, 124.4, 125.4, 126.6, 131.2, 133.5, 134.7, 135.5, 137.1, 138.1, 150.1, 150.8, 178.7, 187.7 ppm; IR (ATR): ν 3221 (br), 3039 (br), 1608, 1550, 1415, 1242, 1114 cm^{-1}; MS (70 eV): m/z (%) = 317 [M + 1]$^+$ (100), 339 [M + Na]$^+$(30), 355 [M + K]$^+$(10) ; Mp = 198 °C.

(1*E*,4*Z*,6*E*)-5-Hydroxy-1-(1*H*-indol-3-yl)-7-(pyridin-4-yl)hepta-1,4,6-trien-3-one (**3 i**): orange solid (16%); reversed phase column chromatography, t_R = 3.46 min (gradient conditions, 15% acetonitrile in water to 100% acetonitrile, 5 min, flow rate: 1 mLmin^{-1}); ^{1}H NMR (400 MHz, [D$_6$]DMSO): δ = 6.26 (s, 1H), 6.83 (d, J = 15.8 Hz, 1H), 7.18 (d, J = 16.1 Hz, 1H), 7.21–7.28 (m, 2H), 7.49–7.51 (m, 1H), 7.54 (d, J = 16.1 Hz, 1H), 7.75–7.78 (m, 2H), 8.00 (d, J = 15.8 Hz, 1H), 8.01–8.06 (m, 2H), 8.67–8.69 (m, 2H), 11.97 ppm (brs, 1H); ^{13}C NMR (100 MHz, [D$_6$]DMSO): δ = 102.8, 113.0, 113.2, 118.6, 120.7, 121.7, 122.3, 123.3, 125.4, 129.0, 133.8, 135.8, 137.6, 138.1, 142.6, 150.8, 177.3, 188.7 ppm; IR (ATR): ν 3037 (br), 1587, 1545, 1413, 1269, 1116 cm^{-1}; MS (70 eV): m/z (%) = 317 [M + 1]$^+$(100), 339 [M + Na]$^+$(10); Mp = 178 °C.

(1*E*,4*Z*,6*E*)-5-Hydroxy-1-(1*H*-indol-3-yl)-7-(pyridin-2-yl)hepta-1,4,6-trien-3-one (**3 j**): orange solid (19%); reversed phase column chromatography, tR = 3.56 min (gradient conditions, 15% acetonitrile in water to 100% acetonitrile, 5 min, flow rate: 1 mLmin^{-1}); ^{1}H NMR (400 MHz, [D$_6$]DMSO): δ = 6.31 (s, 1H), 6.82 (d, J = 15.7 Hz, 1H), 7.21 (d, J = 15.5 Hz, 1H), 7.20–7.27 (m, 2H), 7.38 (ddd, J = 7.6, 4.8, 0.9 Hz, 1H), 7.49–7.51 (m, 1H), 7.58 (d, J = 15.5 Hz, 1H), 7.70 (dd, J = 7.7, 0.9 Hz, 1H), 7.86 (ddd, J = 7.7, 7.6, 1.4 Hz, 1H), 8.01 (d, J = 15.7 Hz, 1 H), 8.01–8.03 (m, 2H), 8.66 (dd, J = 4.8, 1.4 Hz, 1H), 11.93 ppm (s, 1H); ^{13}C NMR (100 MHz, [D$_6$]DMSO): δ = 102.7, 113.0, 113.2, 118.8, 120.7, 121.6, 123.3, 124.6, 125.0, 125.5, 127.8, 133.6, 137.4, 137.6, 137.7, 138.0, 150.5, 153.4, 177.5, 188.7 ppm; δ = IR (ATR): ν 3159 (br), 1612, 1575, 1483, 1442, 1288, 1174 cm^{-1}; MS (70 eV): m/z (%) = 317 [M + 1]$^+$(100), 339 [M + Na]$^+$(20); Mp = 204 °C.

(1*E*,4*Z*,6*E*)-5-Hydroxy-1-(1*H*-indol-3-yl)-7-(quinolin-2-yl)hepta-1,4,6-trien-3-one (**3 k**): orange solid (43%); reversed phase column chromatography, t_R = 3.84 min (gradient conditions, 15% acetonitrile in water to 100% acetonitrile, 5 min, flow rate: 1 mLmin^{-1}); ^{1}H NMR (400 MHz, [D$_6$]DMSO): δ = 6.40 (s, 1H), 6.84 (d, J = 15.8 Hz, 1H), 7.22–7.28 (m, 2H), 7.38 (d, J = 15.8 Hz, 1H), 7.50 (d, J = 7.2 Hz, 1H), 7.64 (dd, J = 7.3, 7.3 Hz, 1H), 7.72 (d, J = 15.8 Hz, 1H), 7.81 (dd, J = 7.4, 7.4 Hz, 1H), 7.95 (d, J = 8.5 Hz, 1H), 7.99–8.05 (m, 4H), 8.01 (d, J = 15.8 Hz, 1H), 8.44 (d, J = 8.5 Hz, 1H), 11.95 ppm (s, 1H); ^{13}C NMR (100 MHz, [D$_6$]DMSO): δ = 103.0, 113.0, 113.3, 118.9, 120.7, 121.6, 121.7, 123.3, 125.5, 127.6, 128.1, 128.4, 129.6, 129.7, 130.7, 133.7, 137.4, 137.7, 138.0, 138.1, 148.1, 154.1, 176.9, 189.1 ppm; IR (ATR): ν 3184 (br), 1598, 1564, 1502, 1226, 1116 cm^{-1}; MS (70 eV): m/z (%) = 367 [M + 1]$^+$(100), 389 [M + Na]$^+$(5); Mp = 204 °C.

(1*E*,4*Z*,6*E*)-5-Hydroxy-1-(1*H*-indol-3-yl)-7-(1H-pyrrol-2-yl)hepta-1,4,6-trien-3-one (**3 l**): dark-red solid (62%); reversed phase column chromatography, t_R = 3.56 min (gradient conditions, 15% acetonitrile in water to 100% acetonitrile, 5 min, flow rate: 1 mLmin^{-1}); ^{1}H NMR (400 MHz, [D$_4$]MeOD): δ = 5.87 (s, 1H), 6.23 (dd, J = 3.4, 2.8 Hz, 1H), 6.37 (d, J = 15.7 Hz, 1H), 6.55 (dd, J = 3.4, 0.8 Hz, 1H), 6.70 (d, J = 15.8 Hz, 1H), 6.97–6.98 (m, 1H), 7.19–7.26 (m, 2H), 7.44–7.46 (m, 1H), 7.50 (d, J = 15.7 Hz, 1H), 7.68 (s, 1H), 7.92 (d, J = 15.8 Hz, 1H), 7.95–7.96 ppm (m, 1H); ^{13}C NMR (100 MHz, [D$_4$]MeOD): δ = 110.1, 111.8, 113.4, 114.2, 116.7, 118.2, 119.7, 120.7, 122.5, 122.8, 125.3, 129.4, 130.0, 130.5, 134.9, 137.9, 182.5, 184.3 ppm; δ = IR (ATR): ν 3367 (br), 3244 (br), 1602, 1566, 1496, 1369, 1242 cm^{-1}; MS (70 eV): m/z (%) = 305 [M + 1]$^+$(100) 327 [M + Na]$^+$(40); Mp = 172 °C.

(1*E*,4*Z*,6*E*)-5-Hydroxy-1-(1*H*-indol-3-yl)-7-(thiophen-2-yl)hepta-1,4,6-trien-3-one (**3 m**): bright red solid (69%); reversed phase column chromatography, t_R = 3.84 min (gradient conditions, 15% acetonitrile in water to 100% acetonitrile, 5 min, flow rate: 1 mLmin^{-1}); ^{1}H NMR (400 MHz, [D$_6$]DMSO): δ = 6.18 (s, 1H), 6.55 (d, J = 15.6 Hz, 1H), 6.75 (d, J = 15.8 Hz, 1H), 7.16 (dd, J = 5.0, 3.6 Hz, 1H), 7.20–7.27 (m, 2H), 7.49–7.51 (m, 2H), 7.71 (d, J = 5.0 Hz, 1H), 7.75 (d, J = 15.6 Hz, 1H), 7.95 (d, J = 15.8 Hz, 1H), 7.99–8.01 (m, 2H), 11.89 ppm (s, 1H); ^{13}C NMR (100 MHz, [D$_6$]DMSO): δ = 101.5, 113.0, 113.2, 118.5, 120.6, 121.6, 123.2, 123.4, 125.4, 129.1, 129.8, 131.8, 132.1, 133.2, 136.5, 138.0, 140.6, 179.7, 186.6 ppm; IR (ATR): ν 3221 (br), 1606, 1502, 1359, 1288, 1242, 1115 cm^{-1}; MS (70 eV): m/z (%) = 322 [M + 1]$^+$(100), 343 [M + Na]$^+$(35); Mp = 188 °C.

Representative Procedure for the Synthesis of Pyrazole-Based Non-Symmetrical Nitrogen-Containing Curcuminoids 4 a–d.

The synthesis of 2-methoxy-4-{(*E*)-2-[5-((*E*)-2-(pyridin-3-yl)vinyl)-1*H*-pyrazol-3-yl]vinyl}phenol **4 a** will be described as a representative example for the synthesis of pyrazole-based non-symmetrical nitrogen-containing curcuminoids **4 a–d**. The reaction conditions for the synthesis of analogues **4 b–d** can be found in Table 3.

(1*E*,4*Z*,6*E*)-5-Hydroxy-1-(4-hydroxy-3-methoxyphenyl)-7-(pyridin-3-yl)hepta-1,4,6-triene-3-one **3 a** (1 mmol, 323.25 mg) was dissolved in 7.5 mL acetic acid, after which 5 equivalents hydrazine hydrate (5 mmol, 0.24 mL) were added. The reaction mixture was stirred for 1 h at reflux conditions. After cooling down, the reaction mixture was diluted in 10 mL ethyl acetate and washed with a saturated solution of sodium bicarbonate (3 × 5 mL). The organic phase was washed with water, dried over $MgSO_4$, filtrated and evaporated under reduced pressure. Purification by means of reversed phase column chromatography (acetonitrile/water, gradient conditions from 15 to 100%), afforded 2-methoxy-4-{(*E*)-2-[5-((*E*)-2-(pyridin-3-yl)vinyl)-1*H*-pyrazol-3-yl]vinyl}phenol **4 a** (239.37 mg, 75%).

2-Methoxy-4-{(*E*)-2-[5-((*E*)-2-(pyridin-3-yl)vinyl)-1*H*-pyrazol-3-yl]vinyl}phenol (**4 a**): beige solid (75%); reversed phase column chromatography, t_R = 3.04 min (gradient conditions, 15% acetonitrile in water to 100% acetonitrile, 5 min, flow rate: 1 mLmin^{-1}); ^{1}H NMR (400 MHz, [D$_6$]DMSO): δ = 3.84 (3H, s), 6.72 (1H, s), 6.78 (1H, d, J = 8.2 Hz), 6.94 (1H, d, J = 16.0 Hz), 6.94 (1H, dd, J = 8.2, 1.7 Hz), 7.08 (1H, d, J = 16.0 Hz), 7.15 (1H, d, J = 1.7 Hz), 7.17 (1H, d, J = 16.1 Hz), 7.26 (1H, d, J = 16.1 Hz), 7.40 (1H, dd, J = 7.9, 4.4 Hz), 8.03 (1H, dt, J = 7.9, 1.6 Hz), 8.46 (1H, d, J = 4.4 Hz), 8.73 (1H, d, J = 1.6 Hz), 9.16 (1H, brs), 13.00 ppm (1H, brs); ^{13}C NMR (100 MHz, [D$_6$]DMSO): δ = 56.0, 100.6, 110.0, 116.1, 120.1, 124.3, 125.9, 128.6, 130.4, 133.0, 147.4, 148.4, 148.6, 148.9 ppm; IR (ATR): ν 3360 (br), 3244 (br), 1641, 1510, 1277, 957 cm^{-1}; MS (70 eV): m/z (%) = 320 [M + 1]$^+$ (100); Mp = 208 °C.

2-Methoxy-4-{(*E*)-2-[5-((*E*)-2-(pyridin-4-yl)vinyl)-1*H*-pyrazol-3-yl]vinyl}phenol (**4 b**): pale green-yellow solid (79%); reversed phase column chromatography, t_R = 3.05 min (gradient conditions, 15% acetonitrile in water to 100% acetonitrile, 5 min, flow rate: 1 mLmin^{-1}); ^{1}H NMR (400 MHz, [D$_6$]DMSO): δ = 3.82 (s, 3H), 6.75 (s, 1H), 6.76 (d, J = 7.7 Hz, 1H), 6.91 (d, J = 17.1 Hz, 1H), 6.92 (d, J = 7.7 Hz, 1H), 7.08 (d, J = 17.1 Hz, 1H), 7.12 (d, J = 16.7 Hz, 1H), 7.12 (s, 1H), 7.41 (d, J = 16.7 Hz, 1H), 7.53 (d, J = 5.8 Hz, 2H), 8.54 ppm (d, J = 5.8 Hz, 2H); ^{13}C NMR (100 MHz, [D$_6$]DMSO): δ = 56.0, 101.0, 110.0, 114.3, 116.2, 120.8, 121.1, 124.6, 126.8, 127.8, 130.8, 144.6, 148.6, 150.5 ppm; IR (ATR): ν 3176 (br), 3080 (br), 1587, 1510, 1267, 1118 cm^{-1}; MS (70 eV): m/z (%) = 320 [M + 1]$^+$ (100); Mp = 180 °C.

2-Methoxy-4-{(*E*)-2-[5-((*E*)-2-(isoquinolin-5-yl)vinyl)-1*H*-pyrazol-3-yl]vinyl}phenol (**4 c**): Light-brown solid (41%); reversed phase column chromatography, t_R = 3.21 min (gradient conditions, 15%

© 2019 The Authors. Published by Wiley-VCH Verlag GmbH & Co. KGaA

acetonitrile in water to 100% acetonitrile, 5 min, flow rate: 1 mLmin^{-1}); ^{1}H NMR (400 MHz, [D$_6$]DMSO): δ = 3.85 (3H, s), 6.79 (1H, d, *J* = 8.1 Hz), 6.94 (1H, brs), 6.96 (1H, dd, *J* = 8.1, 1.3 Hz), 6.97 (1H, d, *J* = 16.5 Hz), 7.09 (1H, d, *J* = 16.5 Hz), 7.17 (1H, d, *J* = 1.3 Hz), 7.29 (1H, d, *J* = 16.3 Hz), 7.72 (1H, dd, *J* = 7.9, 7.5 Hz), 7.96 (1H, d, *J* = 16.3 Hz), 8.08 (1H, d, *J* = 7.9 Hz), 8.17 (1H, d, *J* = 7.5 Hz), 8.25 (1H, d, *J* = 6.0 Hz), 8.60 (1H, d, *J* = 6.0 Hz), 9.35 ppm (1H, s); ^{13}C NMR (100 MHz, [D$_6$]DMSO): δ = 56.0, 110.0, 116.1, 116.9, 120.6, 124.2, 127.0, 127.9, 129.1, 130.4, 133.5, 143.6, 147.3, 148.4, 153.5 ppm; IR (ATR): ν 3179 (br), 2932 (br), 1584, 1514, 1277 cm^{-1}; MS (70 eV): m/z (%) = 370 [M + 1]$^+$ (100), 282 (20); Mp = 214 °C.

3-{(*E*)-2-[5-((*E*)-2-(thiophen-2-yl)vinyl)-1*H*-pyrazol-3-yl]vinyl}-1*H*-indole (**4d**): pale brown solid (80%); reversed phase column chromatography, t_R = 3.53 min (gradient conditions, 15% acetonitrile in water to 100% acetonitrile, 5 min, flow rate: 1 mLmin^{-1}); ^{1}H NMR (400 MHz, [D$_6$]DMSO): δ = 6.70 (s, 1H), 6.84 (d, *J* = 16.2 Hz, 1H), 6.96 (d, *J* = 16.5 Hz, 1H), 7.06–7.08 (m, 1H), 7.12–7.21 (m, 3H), 7.32 (d, *J* = 16.2 Hz, 1H), 7.35 (d, *J* = 16.5 Hz, 1H), 7.43–7.47 (m, 2H), 7.65 (s, 1H), 7.89 (d, *J* = 7.6, 1H), 11.38 (s, 1H), 12.75 ppm (brs, 1H); ^{13}C NMR (100 MHz, [D$_6$]DMSO): δ = 99.2, 111.8, 112.5, 113.6, 119.9, 120.3, 122.3, 122.6, 124.2, 125.5, 125.6, 126.55, 126.60 126.9, 128.5, 137.5, 142.5 ppm; IR (ATR): ν 3178 (br), 1710, 1689, 1550, 1462, 1244 cm^{-1}; MS (70 eV): m/z (%) = 318 [M + 1]$^+$ (100); Mp = 202 °C.

X-Ray Crystal Structural Determinations

For the structure of **4b**, X-ray intensity data were collected at 100 K, on a Rigaku Oxford Diffraction Supernova Dual Source (Cu at zero) diffractometer equipped with an Atlas CCD detector using ω scans and CuKα (λ = 1.54184 Å) radiation. The images were interpreted and integrated with the program CrysAlisPro.[32] Using Olex2,[33] the structure was solved by direct methods using the ShelXS structure solution program and refined by full-matrix least-squares on F^2 using the ShelXL program package.[34] Non-hydrogen atoms were anisotropically refined and the hydrogen atoms in the riding mode and isotropic temperature factors fixed at 1.2 times U(eq) of the parent atoms (1.5 times for methyl and hydroxyl groups). The pyrazole and hydroxyl hydrogen atoms were located from a difference Fourier electron density map.

Crystal data for compound **4b**. $C_{19}H_{17}N_3O_2$, *M* = 319.36, monoclinic, space group $P2_1/n$ (No. 14), *a* = 16.6763(3) Å, *b* = 5.40376(11) Å, *c* = 17.7393(4) Å, β = 96.9999(19)°, *V* = 1586.66(6) Å^3, *Z* = 4, *T* = 100 K, ρ_{calc} = 1.337 g cm^{-3}, μ(Cu–Kα) = 0.718 mm^{-1}, *F*(000) = 672, 26796 reflections measured, 3278 unique (R_{int} = 0.0491) which were used in all calculations. The final *R*1 was 0.0387 (I > 2σ (I)) and *wR*2 was 0.1103 (all data).

CCDC 1877188 contains the supplementary crystallographic data for this paper and can be obtained free of charge via www.ccdc.cam.ac.uk/conts/retrieving.html (or from the Cambridge Crystallographic Data Centre, 12, Union Road, Cambridge CB2 1EZ, UK; fax: +44-1223-336033; or deposit@ccdc.cam.ac.uk).

Biology

General

MEM non-essential amino acid solution (NEAA), 2,2-diphenyl-1-picrylhydrazyl (DPPH), penicillin/streptomycin (P/S), Trolox and 2,7-dichlorofluorescein diacetate were purchased from Sigma-Aldrich, whereas 3-(4,5-dimethylthiazol-2-yl)-2,5-diphenyltetrazolium bromide (MTT) and trypan blue were obtained from Amresco. Trypsin/EDTA solution and Dulbecco's phosphate-buffered saline (PBS-, no calcium and no magnesium) were obtained from Life Technologies and fetal bovine serum (FBS) from Greiner Bio-one. All cell lines, Caco-2 (colorectal adenocarcinoma), HepG2 (hepatocellular carcinoma), CHO (Chinese hamster ovary), HT-29 (colorectal adenocarcinoma) and EA.hy926 (endothelial) were obtained from ATCC. These cell lines were cultivated and maintained in a growth medium containing DMEM + glutamax, 1% NEAA, 1% P/S and 10% fetal bovine serum (FBS). During the MTT experiment, serum-free medium was used to avoid interferences. Each compound or positive control was dissolved in DMSO in order to prepare the 25 mM stock solution for both cytotoxicity and antioxidant tests. The stock solutions were aliquoted and stored in a refrigerator until treatment of the cells.

Cytotoxicity Activity: MTT Experiments

Throughout the experiment, standard procedures were used to maintain all cell lines at 37 °C with 95% humidity and 10% CO_2. The MTT assay was performed to determine the number of viable cells in this assay. Briefly, 20000 cells suspended in the DMEM medium (200 μL) were first inoculated into each well of 96-well microplates and incubated for 24 hours. Then, the medium in each well was removed and an equal volume of serum free medium (200 μL/well) containing either test compounds or positive control (doxorubicin hydrochloride, Dox) at various concentrations was added for 72 hours. Each compound was performed in triplicate. Afterwards, the cell viability was determined by removing 100 μL of medium and adding 20 μL of MTT solution (5 mg/mL in PBS) followed by 2 hours of incubation. Finally, the DMEM medium with MTT solution was then removed and replaced with DMSO to dissolve the formazan crystal. The 96-well microplate was then measured at 570 nm using a Spectramax (Molecular Devices) microplate spectrophotometer. For the data analysis, the percentage of surviving cells after a 72 hours exposure to various concentrations of each test compound was calculated to obtain the IC_{50} value of each compound.

Protein Content (SRB) Analysis

The SRB assay is based on the measurement of cellular proteins. Sulforhodamine B binds electrostatically with basic amino acid residues if the cells are fixed with trichloroacetic acid (TCA) and can be solubilized by weak bases. Because of this quantitative staining capacity of SRB, the assay is used to screen for cytotoxicity and cell density. The cells were seeded at a concentration of 20000 cells per well, incubated for 24 hours and treated with or without (control) compounds. Three days after this treatment the cells were fixed by addition of 50 μL of 50% TCA in Milli-Q water for 1 hour in the cold room, 4 °C. The plate was washed at least 3 times with tap water and dried, after which the cells were stained with an SRB solution (0.4% sulforhodamine B in 1% glacial acetic acid) at 4 °C. After 30 minutes, the plate was rinsed for 5 times with 1% glacial acetic acid and dried. Sequentially, Tris buffer in a concentration of 10 mM was used to re-dissolve the stain. Finally, the absorbance was measured using the microplate spectrophotometer at a wavelength of 490 nm. Each condition was performed in triplicate.

Reactive Oxygen Species (ROS) Assay

The experiments were performed in an incubator at 37 °C with 10% CO2. Seeding of a concentration of 20000 cells per well in a DMEM medium was performed in a black 96-well plate with transparent bottom. After 24 hours, the confluent cells were equally treated with or without the compounds at 10 and 1 μM in serum-free medium (200 μL). Then, after removal of the medium, the cells

© 2019 The Authors. Published by Wiley-VCH Verlag GmbH & Co. KGaA

were washed with PBS buffer followed by the addition of 2′,7′-dichlorofluorescein diacetate (DCFH-DA, 20 μM) for a 30-minute incubation period. Thereafter, the DCFH-DA was removed and the cells were washed with PBS buffer. Afterwards, the DMEM without phenol red medium was added in equal volume for one hour of incubation. Finally, the black 96-well plates were measured for fluorescence with a Gemini XPS Microplate Reader with an excitation of 485 nm and an emission of 535 nm. Afterwards, an SRB assay was applied to the cells as described above, in order to normalize the results, for cell density.

Chemical Antioxidant Capacity: Ferric Reducing Ability of Plasma (FRAP) Assay

An acetate buffer of 300 mM was prepared by adding 3.1 g of sodium acetate trihydrate to 16 mL of acetic acid, which was diluted to 1000 mL with Milli-Q water. The TPTZ (2,4,6-tripyridyl-s-triazine) solution of 10 mM was prepared by adding 0.156 g of TPTZ to 50 mL of ethanol. Lastly, a 20 mM solution of iron(III) chloride hexahydrate was prepared by mixing 0.5404 g of $FeCl_3.6H_2O$ with 2 mL 37% HCl and 98 mL Milli-Q water. The TPTZ and iron solutions were freshly prepared on the day of the assay. These 3 mixtures were added in a 10:1:1 ratio to obtain the FRAP reagent (acetate buffer:TPTZ: $FeCl_3.6H_2O$). Finally, 100 μL of the samples were mixed with 900 μL of the FRAP reagent and after 4 minutes the absorbance was measured at 593 nm in a Spectramax microplate spectrophotometer. Trolox was used as a standard and the FRAP value was calculated as Trolox equivalent (μM) *via* a linear regression of the Trolox standard curve or curcumin standard curve.

Water Solubility Measurement

The shake flask method is commonly used to measure aqueous solubility.[22b,35] The test compounds were first measured for maximum absorbance using the Liquid Chromatography (LC, Agilent 1100 Series LC/MSD type SL mass spectrometer with electrospray ionization (ESI 70 eV)) technique using Ascentis® Express C18, HPLC column 3 cm × 4.6 mm, 2.7 μm (LC method for 5 min at flow rate 1 mL/min during the gradient elution of the combination between water and acetonitrile, 30% to 100% acetonitrile). Afterwards, the standard curves were prepared from various concentrations of the test compounds. In this experiment, a sodium phosphate-buffered solution at pH 6.8 was used to perform the solubility test of each non-symmetrical derivative. The excess of the solid compounds was added into 1 mL of the phosphate-buffered solution (pH 6.8). The experiment was divided into two-time points. The first one was fixed at 90 minutes under a sonicator bath at 37 °C and the second one at 30 minutes under a sonicator bath at 37 °C followed by 23 hours of incubation at 300 rpm and a further 30 minutes' sonication. Both time points of each sample were centrifuged at 14,000 rpm for 5 minutes. Then, all compounds were filtered (0.2 micron) at 37 °C. Subsequently, the solutions were diluted in methanol to avoid the precipitation of the compounds at room temperature as using in previous procedures.[2h,i] Each compound was individually measured at its maximum absorbance. Finally, the solubility values were calculated from the linear equations of each standard curve. The experiment was independently triplicated.

Acknowledgements

The authors are indebted to Ghent University and to the Lotus + Erasmus Mundus Programme of the European Union for financial support. KVH thanks the Hercules Foundation (project AUGE/11/029 "3D-SPACE: 3D Structural Platform Aiming for Chemical Excellence") and the Special Research Fund (BOF) – UGent (project 01N03217) for funding. The authors also would like to thank ir. Sari Deketelaere from Ghent University for her assistance in this manuscript preparation.

Conflict of Interest

The authors declare no conflict of interest.

Keywords: curcumin · cytotoxicity · water solubility · anticancer activity · antioxidant activity

[1] a) S. Singh, *Cell* **2007**, *130*, 765–768; b) J. Epstein, I. R. Sanderson, T. T. Macdonald, *Br. J. Nutr.* **2010**, *103*, 1545–1557; c) A. Goel, B. B. Aggarwal, *Nutr. Cancer* **2010**, *62*, 919–930.

[2] a) R. Kuttan, P. Bhanumathy, K. Nirmala, M. C. George, *Cancer Lett.* **1985**, *29*, 197–202; b) A. J. Ruby, G. Kuttan, K. D. Babu, K. N. Rajasekharan, R. Kuttan, *Cancer Lett.* **1995**, *94*, 79–83; c) M. L. Kuo, T. S. Huang, J. K. Lin, *Biochim. Biophys. Acta* **1996**, *1317(2)*, 95–100; d) K. Mehta, P. Pantazis, T. McQueen, B. B. Aggarwal, *Anti-Cancer Drugs* **1997**, *8*, 470–481; e) K. Singletary, C. MacDonald, M. Iovinelli, C. Fisher, M. Wallig, *Carcinogenesis* **1998**, *19*, 1039–1043; f) T. Kawamori, R. Lubet, V. E. Steele, G. J. Kelloff, R. B. Kaskey, C. V. Rao, B. S. Reddy, *Cancer Res.* **1999**, 59; g) R. De Vreese, C. Grootaert, S. D'hoore, A. Theppawong, S. Van Damme, M. Van Bogaert, J. Van Camp, M. D'hooghe, *Eur. J. Med. Chem.* **2016**, *123*, 727–736; h) A. Theppawong, R. De Vreese, L. Vannecke, C. Grootaert, J. Van Camp, M. D'hooghe, *Bioorg. Med. Chem. Lett.* **2016**, *26*, 5650–5656; i) A. Theppawong, T. Van de Walle, C. Grootaert, M. Bultinck, T. Desmet, J. Van Camp, M. D'hooghe, *ChemistryOpen* **2018**, *7*, 381–392.

[3] a) H. P. Ammon, H. Safayhi, T. Mack, J. Sabieraj, *J. Ethnopharmacol.* **1993**, *38*, 113–119; b) Y. X. Xu, K. R. Pindolia, N. Janakiraman, R. A. Chapman, S. C. Gautam, *Hematopathol. Mol. Hematol.* **1997**, *11*, 49–62.

[4] a) A. C. Reddy, B. R. Lokesh, *Mol. Cell. Biochem.* **1992**, *111*, 117–124; b) Sreejayan, M. N. Rao, *J. Pharm. Pharmacol.* **1994**, *46*, 1013–1016.

[5] J. A. Makawana, M. P. Patel, R. G. Patel, *Chin. Chem. Lett.* **2012**, *23*, 427–430.

[6] a) R. C. Reddy, P. G. Vatsala, V. G. Keshamouni, G. Padmanaban, P. N. Rangarajan, *Biochem. Biophys. Res. Commun.* **2005**, *326*, 472–474; b) D. N. Nandakumar, V. A. Nagaraj, P. G. Vathsala, P. Rangarajan, G. Padmanaban, *Antimicrob. Agents Chemother.* **2006**, *50*, 1859–1860; c) L. Cui, J. Miao, L. Cui, *Antimicrob. Agents Chemother.* **2007**, *51*, 488–494; d) S. Mishra, K. Karmodiya, N. Surolia, A. Surolia, *Bioorg. Med. Chem.* **2008**, *16*, 2894–2902.

[7] B. L. Zhao, X. J. Li, R. G. He, S. J. Cheng, W. J. Xin, *Cell Biophys.* **1989**, *14*, 175–185.

[8] a) Y. J. Wang, M. H. Pan, A. L. Cheng, L. I. Lin, Y. S. Ho, C. Y. Hsieh, J. K. Lin, *J. Pharm. Biomed. Anal.* **1997**, *15*, 1867–1876; b) H. Hatcher, R. Planalp, J. Cho, F. M. Torti, S. V. Torti, *Cell. Mol. Life Sci.* **2008**, 65; c) M. H. Leung, T. W. Kee, *Langmuir* **2009**, *25*, 5773–5777.

[9] K. M. Nelson, J. L. Dahlin, J. Bisson, J. Graham, G. F. Pauli, M. A. Walters, *J. Med. Chem.* **2017**, 1620–1637.

[10] a) M. H. Pan, T. M. Huang, J. K. Lin, *Drug Metab. Dispos.* **1999**, *27*, 486–494; b) P. Anand, A. B. Kunnumakkara, R. A. Newman, B. B. Aggarwal, *Mol. Pharm.* **2007**, *4*, 807–818.

[11] a) R. A. Sharma, H. R. McLelland, K. A. Hill, C. R. Ireson, S. A. Euden, M. M. Manson, M. Pirmohamed, L. J. Marnett, A. J. Gescher, W. P. Steward, *Clin. Cancer Res.* **2001**, *7*, 1894–1900; b) A. Kunwar, A. Barik, B. Mishra, K. Rathinasamy, R. Pandey, K. I. Priyadarsini, *Biochim. Biophys. Acta* **2008**, *1780*, 673–679.

[12] a) G. Shoba, D. Joy, T. Joseph, M. Majeed, R. Rajendran, P. S. S. R. Srinivas, *Planta Med.* **1998**, *64*, 353–356; b) A. S. Strimpakos, R. A. Sharma, *Antioxid. Redox Signaling* **2008**, *10*, 511–545; c) S. K. Vareed, M. Kakarala, M. T. Ruffin, J. A. Crowell, D. P. Normolle, Z. Djuric, D. E. Brenner, *Cancer Epidemiol. Biomarkers Prev.* **2008**, *17*, 1411–1417; d) S. C. Gupta, S. Patchva, B. B. Aggarwal, *AAPS J.* **2013**, *15*, 195–218.

© 2019 The Authors. Published by Wiley-VCH Verlag GmbH & Co. KGaA

[13] A. Vyas, P. Dandawate, S. Padhye, A. Ahmad, F. Sarkar, *Curr. Pharm. Des.* **2013**, *19*, 2047–2069.
[14] a) J. Das, S. Pany, S. Panchal, A. Majhi, G. M. Rahman, *Bioorg. Med. Chem.* **2011**, *19*, 6196–6202; b) M. J. Ahsan, H. Khalilullah, S. Yasmin, S. S. Jadav, J. Govindasamy, *BioMed Res. Int.* **2013**, *2013*, 239354; c) S. Chakraborti, G. Dhar, V. Dwivedi, A. Das, A. Poddar, G. Chakraborti, G. Basu, P. Chakrabarti, A. Surolia, B. Bhattacharyya, *Biochemistry* **2013**, *52*, 7449–7460.
[15] a) H. R. Puneeth, H. Ananda, K. S. S. Kumar, K. S. Rangappa, A. C. Sharada, *Med. Chem. Res.* **2016**, *25*, 1842–1851; b) R. Sribalan, G. Shakambari, G. Banuppriya, P. Varalakshmi, E. R. Subramanian, S. Sudhakar, V. Padmini, *ChemistrySelect* **2017**, *2*, 1122–1128; c) M. Ahmed, M. A. Qadir, A. Hameed, M. Imran, M. Muddassar, *Chem. Biol. Drug Des.* Des **2018**, *91*, 338–343.
[16] D. L. Flynn, T. R. Belliotti, A. M. Boctor, D. T. Connor, C. R. Kostlan, D. E. Nies, D. F. Ortwine, D. J. Schrier, J. C. Sircar, *J. Med. Chem.* **1991**, *34*, 518–525.
[17] a) J. Ishida, H. Ohtsu, Y. Tachibana, Y. Nakanishi, K. F. Bastow, M. Nagai, H.-K. Wang, H. Itokawa, K.-H. Lee, *Bioorg. Med. Chem.* **2002**, *10*, 3481–3487; b) J. S. Shim, D. H. Kim, H. J. Jung, J. H. Kim, D. Lim, S. K. Lee, K. W. Kim, J. W. Ahn, J. S. Yoo, J. R. Rho, J. Shin, H. J. Kwon, *Bioorg. Med. Chem.* **2002**, *10*, 2987–2992.
[18] H. J. J. Pabon, *Recl. Trav. Chim. Pays-Bas* **1964**, *83*, 379–386.
[19] a) Y. H. Ahn, J. S. Yoo, *Anal. Sci.* **2001**, *17*, 893–895; b) E. V. Dalessandro, H. P. Collin, L. G. L. Guimarães, M. S. Valle, J. R. Pliego, *J. Phys. Chem. B* **2017**, *121*, 5300–5307.
[20] a) S. Sharma, M. K. Gupta, A. K. Saxena, P. M. S. Bedi, *Bioorg. Med. Chem.* **2015**, *23*, 7165–7180; b) H. Singh, M. Kumar, K. Nepali, M. K. Gupta, A. K. Saxena, S. Sharma, P. M. S. Bedi, *Eur. J. Med. Chem.* **2016**, *116*, 102–115; c) H. Singh, J. V. Singh, M. K. Gupta, A. K. Saxena, S. Sharma, K. Nepali, P. M. S. Bedi, *Bioorg. Med. Chem. Lett.* **2017**, *27*, 3974–3979.
[21] M. W. Amolins, L. B. Peterson, B. S. J. Blagg, *Bioorg. Med. Chem.* **2009**, *17*, 360–367.
[22] a) L. Zhou, L. Yang, S. Tilton, J. Wang, *J. Pharm. Sci.* **2007**, *96*, 3052–3071; b) E. Baka, J. E. Comer, K. Takacs-Novak, *J. Pharm. Biomed. Anal.* **2008**, *46*, 335–341.
[23] a) V. P. Menon, A. R. Sudheer, *Adv. Exp. Med. Biol.* **2007**, *595*, 105–125; b) P. Somparn, C. Phisalaphong, S. Nakornchai, S. Unchern, N. P. Morales, *Biol. Pharm. Bull.* **2007**, *30*, 74–78.
[24] a) I. F. F. Benzie, J. J. Strain, *Anal. Biochem.* **1996**, *239*, 70–76; b) G. Litwinienko, K. U. Ingold, *J. Org. Chem.* **2004**, *69*, 5888–5896; c) K. Thaipong, U. Boonprakob, K. Crosby, L. Cisneros-Zevallos, D. Hawkins Byrne, *J. Food Compos. Anal.* **2006**, *19*, 669–675; d) T. Ak, İ. Gülçin, *Chem.-Biol. Interact.* **2008**, *174*, 27–37.
[25] C. F. Thorn, C. Oshiro, S. Marsh, T. Hernandez-Boussard, H. McLeod, T. E. Klein, R. B. Altman, *Pharmacogenet. Genomics* **2011**, *21*, 440–446.
[26] a) H. Pelicano, D. Carney, P. Huang, *Drug Resist. Updates* **2004**, *7*, 97–110; b) G. Waris, H. Ahsan, *J. Carcinog.* **2006**, *5*, 14–14.
[27] a) G. Lenaz, C. Bovina, M. D'Aurelio, R. Fato, G. Formiggini, M. L. Genova, G. Giulianol, M. M. Pich, U. Paolucci, G. P. Castelli, B. Ventura, *Ann. N. Y. Acad. Sci.* **2002**, *959*, 199–213; b) B. Van Houten, V. Woshner, J. H. Santos, *DNA Repair* **2006**, *5*, 145–152; c) M. L. Circu, T. Y. Aw, *Free Radical Biol. Med.* **2010**, *48*, 749–762.
[28] a) S.-Y. Sun, *Cancer Biol. Ther.* **2010**, *9*, 109–110; b) M. Halasi, M. Wang, T. S. Chavan, V. Gaponenko, N. Hay, A. L. Gartel, *Biochem. J.* **2013**, *454*, 201–208; c) R. Bavarsad Shahripour, M. R. Harrigan, A. V. Alexandrov, *Brain Behav. Immun.* **2014**, *4*, 108–122.
[29] a) S. J. Duthie, W. T. Melvin, M. D. Burke, *Xenobiotica* **1994**, *24*, 265–279; b) A. Lancon, N. Hanet, B. Jannin, D. Delmas, J. M. Heydel, G. Lizard, M. C. Chagnon, Y. Artur, N. Latruffe, *Drug Metab. Dispos.* **2007**, *35*, 699–703.
[30] A. Fasano, *Physiol. Rev.* **2011**, *91*, 151–175.
[31] I. Lee, J. Yang, J. H. Lee, Y. S. Choe, *Bioorg. Med. Chem. Lett.* **2011**, *21*, 5765–5769.
[32] Rigaku Oxford Diffraction (2015). CrysAlis Pro; Rigaku Oxford Diffraction, Yarnton, England.
[33] O. V. Dolomanov, L. J. Bourhis, R. J. Gildea, J. A. K. Howard, H. Puschmann, *J. Appl. Crystallogr.* **2009**, *42*, 339–341.
[34] a) G. Sheldrick, *Acta Crystallogr. Sect. A* **2008**, *64*, 112–122; b) G. Sheldrick, *Acta Crystallogr. Sect. C* **2015**, *71*, 3–8.
[35] L. Zhou, L. Yang, S. Tilton, J. Wang, *J. Pharm. Sci.* **2007**, *96*, 3052–3071.

Manuscript received: December 13, 2018
Revised manuscript received: February 5, 2019

© 2019 The Authors. Published by Wiley-VCH Verlag GmbH & Co. KGaA